Absorbers as detectors for unbound quantum systems

Sølve Selstø[1]

[1]*Faculty of Technology, Art and Design, Oslo Metropolitan University, NO-0130 Oslo, Norway*

Complex absorbing potentials are frequently employed in quantum calculations. One of the advantages that such absorbers provide is the ability to attenuate outgoing waves in simulations of unbound systems, thus allowing for truncating the numerical domain. Here, we argue that the absorber may also be used to *probe* outgoing waves so that physical information about absorbed particles may be retained. Moreover, under certain conditions the physical information extracted via the absorber is subject to loss in coherence, as is also the case when collapsing the wave function upon measurement. Both these aspects demonstrate clearly how, and when, the effect of introducing a complex absorbing potential corresponds to that of a detector.

I. INTRODUCTION

Several theoretical and numerical studies of quantum systems make use of complex absorbing potentials (CAPs) [1–4]. Arguably, the most frequent application is simulations of unbound systems as they allow for applying truncated numerical domains by attenuating outgoing waves without imposing artifacts such as unphysical reflections. They are also applied in order to determine the characteristics of resonance states and to describe many-particle tunneling decay, see, e.g., Refs. [3, 5–9]. Moreover, CAPs are used to calculate arrival times in quantum systems [10–13]; arrival times may be determined from the loss in the norm of the wave function, the *absorption rate*, that the CAP induces. In this context, CAPs or other non-Hermitian Hamiltonians are typically introduced in order to mimic continuous observation. In the case of strong absorbing potentials, such rates are, in fact, suppressed, which, in turn, is a manifestation of the quantum Zeno effect [14–16]. This is an example of how a quantum system may be manipulated by tailored measurements.

CAPs are usually imposed artificially – with the sole motivation of facilitating numerical implementations. Refs. [13, 17] are exceptions to this rule, however, as they arrive at effective CAPs from more fundamental principles. In the latter case, this is done under very specific conditions, while the former features a very generic approach, one in which a detector is coupled to an environment in order to encompass the irreversible nature of measurement. This, in turn, underlines that detection really is a Markovian process, and the proper framework is that of open quantum systems.

Although works such as Refs. [2, 11, 13, 17–20] highlight the close connection between CAPs and detectors, the actual effect of the CAPs is usually reduced to simply removing parts of the wave function. However, since we know what we remove, we can do better. We can use the CAP in order to *probe* the outgoing waves and, thus, extract physical information about the quantum system in question – physical information such as energy or ejection angle. After all, this is the main purpose of imposing a detector. Moreover, the act of detection imposes loss in coherence. Detector models which incorporate both these aspects are more scarce.

It should be noted that a family of methods for extracting information about unbound quantum particles prior to absorption, see, e.g, Refs. [21–26], or during absorption, see, e.g., Refs. [27–33], have been put forward. As will be apparent in the following, the present approach differ from these in several respects. In the one-particle case, the present scheme may be formulated in a rather straight forward manner in terms of continuous projective measurements. While slightly less straight forward, it may also, along the lines explained in [34], be generalized to any number of particles exposed to any CAP acting as a one-particle operator. In addition to studying how various ways of implementing CAPs may be used in order to probe outgoing waves and determine distribution functions for unbound particles, we will also explain how the CAP characteristics affect the coherence properties of these distributions. This, in turn, provides a clear criterion for when a CAP may be considered to act as a detector.

In the next section the theory is explained – with emphasis on unbound systems with one-particle. Its application is illustrated with two simple examples in Sec. III. The purpose of these numerical examples is to demonstrate how information about unbound particles may be retained despite absorption – and how different absorbers affect the coherence properties. In Sec. III C it is briefly explained how the formalism generalizes to a multi-particle context. The section also features a brief comparison with some other approaches featuring absoprtion/particle removal. Conclusions are drawn in Sec. IV.

II. THEORY

Here we will explain the theory before we illustrate it with two numerical examples. We will also outline how these notions generalize to many-particle systems.

A. Wave function depletion

The evolution of the wave function for a quantum system is dictated by the Schrödinger equation,

$$i\hbar\frac{\mathrm{d}}{\mathrm{d}t}\Psi = H\Psi, \tag{1}$$

or generalizations thereof. The CAP is introduced by replacing the Hermitian Hamiltonian H with an effective non-Hermitian Hamiltonian

$$H_{\mathrm{eff}} = H - i\Gamma, \tag{2}$$

This is a peer reviewed, accepted postprint-version of the following journal article that has been published in Physical Review A: Selstø, Sølve (2022). Absorbers as detectors for unbound quantum systems. Physical Review A (PRA), 106, (*4*). DOI: https://doi.org/10.1103/PhysRevA.106.042213

where the CAP, Γ, may be a local potential, i.e., one that depends on position only, or a non-local one. In any case, it should be chosen such that it only affects the dynamics near the boundary of the numerical domain and leaves the interior region unaffected. Here we will also insist that the Γ-operator is Hermitian and positive semi-definite,

$$\Gamma^\dagger = \Gamma, \quad \text{and} \quad \Gamma \geq 0. \tag{3}$$

This ensures that the norm of the corresponding wave function decreases for a system where there is an overlap between the CAP and the wave function; from one time step to the next, a part of the wave function will be removed. We wish to analyze this part on the fly. In order to arrive at a properly normalized expression we find it instructive to do this in terms of the corresponding pure state density matrix, $\rho = |\Psi\rangle\langle\Psi|$:

$$\rho(t+\Delta t) = \rho(t) - \frac{i}{\hbar}[H,\rho]\Delta t - \frac{1}{\hbar}\{\Gamma,\rho\}\Delta t + \mathcal{O}(\Delta t^2). \tag{4}$$

The part which has been removed from the density matrix during this time step is given by the anti-commutator above. In a context in which only the remainder is under study, a normalization of the density matrix may be imposed, which, in turn, leads to a non-linear master equation for the time evolution [35–37]. Here, on the other hand, we want the trace of ρ to decrease according to Eq. (4). For a single-particle system, the anti-commutator in Eq. (4) adds to an effective one-particle density matrix σ:

$$d\sigma = \frac{1}{\hbar}\{\Gamma,\rho\}\, dt. \tag{5}$$

The notion of σ as a density matrix should not be take too far, however. While it is a Hermitian operator, σ is not in general positive semi-definite.

B. The momentum/energy differential spectrum

Suppose now that we are interested in, e.g., the probability distribution differential in momentum for a single unbound particle, $\partial P/\partial p$. This can be estimated by aggregating the diagonal elements in the momentum eigen states $|p\rangle$:

$$\frac{\mathrm{d}}{\mathrm{d}t}\frac{\partial P}{\partial p} = \langle p|\frac{d\sigma}{dt}|p\rangle = \frac{1}{\hbar}\langle p|\{\Gamma,\rho\}|p\rangle, \tag{6}$$

or, alternatively, in terms of projective measurements:

$$\frac{\partial P}{\partial p} = \int_{t=0}^{t=\infty} \mathrm{Tr}\ (|p\rangle\langle p| d\sigma)\,. \tag{7}$$

For the CAP, the simplest and, arguably, most natural choice is that of a local potential, i.e., one that is diagonal in position x:

$$\Gamma_x = \int dx\ \gamma(x)|x\rangle\langle x|, \tag{8}$$

where $|x\rangle$ are position eigen states and the CAP position function $\gamma(x)$ is zero in the interior of the domain and positive closer to the boundary of the numerical domain. Here '$\int dx$' is to be taken as the definite integral over all space, in all dimensions. Now, according to Eq. (6) or (7), the momentum-differential probability distribution of the unbound part of the wave function reads

$$\frac{\partial P}{\partial p} = \int_{t=0}^{t=\infty} \mathrm{Tr}\ (|p\rangle\langle p| d\sigma_x) = \tag{9}$$
$$\frac{2}{\hbar}\mathrm{Re}\int_0^\infty dt\,[\mathcal{F}\{\Psi(x;t)\}(p)]^*\,\mathcal{F}\{\gamma(x)\Psi(x;t)\}(p)$$

where $\mathcal{F}$ is the Fourier transform. There may, of course, be other physical quantities of interest than momentum; in Eq. (6) we may very well substitute the momentum projections with projection onto eigen states of other physical observables such as energy or, as we will address in Sec. II C, position. While the CAP may affect the physical system by inducing artificial reflections, Eq. (9) should at least produce the actual asymptotic distribution of the unbound quantum particle in the limit that the CAP function vanishes, $\gamma \to 0^+$.

Note that Eq. (9) provides a *coherent* sum of absorbed contributions obtained at different times; a wave contribution absorbed at a specific time may add constructively or destructively to waves aggregated from earlier absorption. Another, related observation is the fact that the distribution does not only depend on the overlap between the CAP and the wave function, it also depends on the wave function beyond the CAP region. Thus, it is crucial that the support of the states we project onto is not limited to the CAP region.

Also when it comes to the CAP itself, we are not restricted to one that is diagonal in position. We could choose one that is diagonal in momentum or energy instead. Such a CAP would not be given by any local potential. Examples of non-local CAPs seen in literature are *the Transformative CAP* [38, 39], *the Reflection-Free CAP* [40] or *Infinite Range Exterior Complex Scaling* [41]. In our context, we insist that the CAP remains Hermitian, cf. Eq. (3); otherwise, the physics of the particle undergoing absorption is altered in an artificial way. We also insist that the CAP is written in terms of projections as in Eq. (8). However, a straight forward replacement of the position x with the momentum p in Eq. (8) is not adequate as such an implementation would introduce absorption to the entire domain, including the inner interaction region. We propose the following energy absorber:

$$\Gamma_\varepsilon = \int d\varepsilon\ \mu(\varepsilon)|\varphi_\varepsilon\rangle\langle\varphi_\varepsilon|, \tag{10}$$

where the $|\varphi_\varepsilon\rangle$-s are energy normalized eigen functions of the Hamiltonian

$$H_\varepsilon = H + V_\varepsilon(x) \quad \text{where} \quad V_\varepsilon(x) = \begin{cases} \infty, & x \in D_\mathrm{I} \\ 0, & x \notin D_\mathrm{I} \end{cases}. \tag{11}$$

Here, D_I is the interior of the numerical domain; typically it is the given by $|x| \leq R$ for some finite distance R from the origin. With this the eigen functions $\varphi_p(x) = \langle x|\varphi_p\rangle$ are only supported for $x \notin D_\mathrm{I}$. Correspondingly, the CAP of Eq. (10) is both energy and position dependent, contrary to

the strictly position-dependent CAP of Eq. (8). The positive CAP function $\mu(\varepsilon)$, however, is purely energy dependent.

In obtaining the momentum or energy distribution using the CAP of Eq. (10), we will, instead of using the momentum basis, conveniently project onto the $|\varphi_\varepsilon\rangle$ basis, in which the CAP is diagonal:

$$\frac{\partial P}{\partial \varepsilon} = \int_{t=0}^{t=\infty} \mathrm{Tr}\left(|\varphi_\varepsilon\rangle\langle\varphi_\varepsilon| d\sigma_\varepsilon\right) = \frac{2}{\hbar}\int_0^\infty dt\ \mu(\varepsilon)|\langle\varphi_\varepsilon|\Psi(t)\rangle|^2. \tag{12}$$

We note that, contrary to Eq. (9), this integral is *incoherent* and manifestly non-negative. Moreover, it only features contributions from projection onto states which are supported in the CAP region exclusively. Again, the correct, asymptotic distribution should be obtained by extrapolating the strength of the CAP function, in this case $\mu(\varepsilon)$, to zero. However, as we will see, spectra obtained with finite-valued $\mu(\varepsilon)$ are also of interest as it allows us to simulate detection.

C. Angular distribution

In addition to energy/momentum differential distributions, distributions differential in position, or rather, *direction* are also of interest experimentally. For a three-dimensional system we may write the position eigen state $|x\rangle$ in terms of spherical coordinates as $|r, \Omega\rangle$ and introduce the additional assumption on the local CAP of Eq. (8) that it is isotropic:

$$\Gamma_r = \int r^2 dr d\Omega\ \gamma(r)|r,\Omega\rangle\langle r,\Omega|. \tag{13}$$

As in the case of Eq. (12), the position distribution obtained from the position diagonal CAP of Eq. (13) becomes an incoherent integral. As the distribution in radial distance r is usually less interesting than the distribution in Ω, we integrate out the r-dependence and arrive at

$$\frac{\partial P}{\partial \Omega} = \frac{2}{\hbar}\int_0^\infty dt\ \int_0^\infty r^2 dr\ \gamma(r)|\Psi(r,\Omega;t)|^2. \tag{14}$$

The analogous expression in two-dimensional polar coordinates reads

$$\frac{\partial P}{\partial \theta} = \frac{2}{\hbar}\int_0^\infty dt\ \int_0^\infty r dr\ \gamma(r)|\Psi(r,\theta;t)|^2. \tag{15}$$

III. NUMERICAL EXAMPLES

In the following we will illustrate the approaches outlined above to absorption and analysis of two particular unbound one-particle systems. As they are both rather simple and generic, they serve well to illustrate the scheme presented here – with particular emphasis on the close correspondence between detectors and absorbers.

A. Energy spectra for a dynamic one-dimensional system

In our first example, which is one-dimensional, a particle is initially trapped in the ground state of a confining potential $V(x)$, which features a finite number of bound states and a continuum. The particle is exposed to an explicitly time-dependent perturbation; the total (Hermitian) Hamiltonian of the system reads

$$H = -\frac{\hbar^2}{2m}\frac{d^2}{dx^2} + V(x) + qE(t)x, \tag{16}$$

where q is the charge of the particle and

$$E(t) = E_{\mathrm{Pulse}}(t) + E_{\mathrm{Pulse}}(t - T - \tau) \quad \text{where} \tag{17a}$$

$$E_{\mathrm{Pulse}}(t) = \begin{cases} E_0 \sin^2\left(\frac{\pi}{T}t\right)\sin(\omega t), & 0 \le t \le T \\ 0, & \text{otherwise} \end{cases}. \tag{17b}$$

The system may serve as a model atom exposed to two consecutive laser pulses.

The time-dependent Schrödinger equation, Eq. (1), is solved with the effective Hamiltonian of Eq. (2) with the Hermitian part given by Eq. (16). First we employ a local CAP, cf. Eq. (8) with a square CAP function:

$$\gamma(x) = \begin{cases} \gamma_0(x-R)^2, & |x| > R \\ 0, & \text{otherwise} \end{cases}. \tag{18}$$

The interference between outgoing wave components liberated at different times causes a rich structure in the emerging energy distribution of the unbound particle. The left column of Fig. 1 shows this distribution calculated by using Eq. (9). It is plotted against energy rather than momentum. In the CAP region, the confining potential may safely be neglected so that $\varepsilon = p^2/2m$; projecting onto eigen states of the (Hermitian) Hamiltonian rather than plane waves does not alter the results.

We use units defined by choosing $\hbar$, m and $-q$ as the unit of their respective quantities. In these units, i.e., atomic units (a.u.), the confining potential, which is a negative Gaussian, has the depth $V_0 = 0.6$ and the width $\sigma_V = 3$. The corresponding ground state energy is -0.48. The time dependent perturbation is characterized by the strength $E_0 = 2$, the angular frequency $\omega = 1$, and the delay τ between the pulses is 5 time units. Each pulse has a duration corresponding to ten optical cycles, and the CAP onset $R = 200$ length units.

The energy spectra are calculated using various absorber strengths γ_0. It is striking to see that not only does the spectrum converge as the strength of the CAP function decreases; apart from the low energy region, it is virtually independent of the CAP strength. This feature does in no way rely on the specific shape of the CAP function; other choices than the one of Eq. (18) display the same behaviour (not shown). The discrepancies we see at low energies are clearly unphysical, not only because of the γ_0 dependence, but also because they produce "negative probabilities". This undesired feature, which diminish with decreasing γ_0, seems to be related to the fact that hard absorption does induce artificial reflections [11].

With the perturbation of Eqs. (17) interpreted as an external electric field, the structure seen in the upper panels of Fig. 1

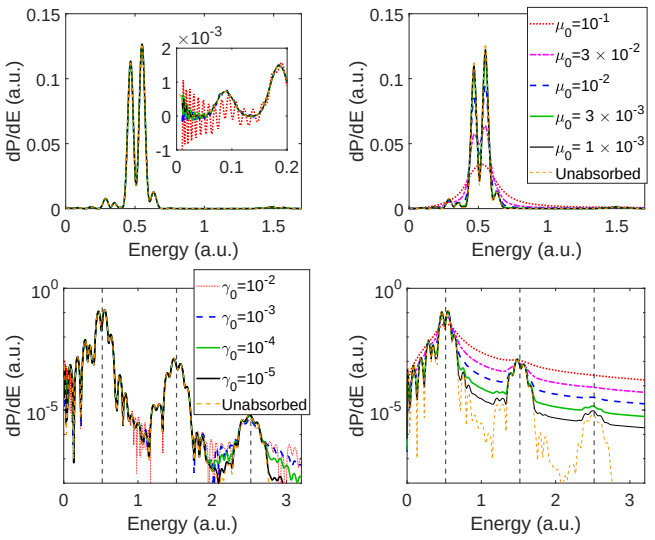

FIG. 1: Left column: Energy distribution from the unbound part of the wave function obtained from a local CAP. Right column: Energy distributions calculated for the same system albeit with an energy CAP. In the latter case, both analysing the outgoing waves and expressing the CAP is done in terms of projections onto eigen states which are only supported in the CAP region. The spectra are plotted for various CAP strengths, be it diagonal in position, γ_0 in Eq. (8), or energy, μ_0 in Eq. (10). The upper panels display the spectra with a linear axis while the lower ones have a logarithmic y-axis. The energy spectrum obtained by conventional means, without absorption, is also included for comparison. The vertical dashed lines in the lower panels indicates $n \cdot \hbar\omega$ for $n = 1, 2$ and 3.

corresponds to absorption of one photon. With a logarithmic y-axis, we also clearly see structures corresponding to absorption of two and three photons as well (lower panels). A somewhat stronger γ_0-dependence is seen at the multi-photon peaks. For a direct comparison, we have also calculated the energy spectrum obtained by conventional means, i.e., by projecting the unabsorbed wave function onto the appropriate scattering states, in the panes of Fig. 1.

It may appear less than intuitive that we, in fact, arrive at spectra which agree very well with the correct one using projection onto plane waves, which, contrary to the appropriate scattering states, does not take the nature of the potential V into account. Of course, the analysis is based on the overlap between the CAP operator and the absorbed density matrix; the potential may safely be neglected in the CAP region. However, as discussed in regard to Eq. (9), the resulting formula depends on the overlap between the wave function and the scattering states in the inner region as well. As it turns out, the analysis is quite insensitive to the *shape* of the scattering states in the inner region. But the ability to preserve coherence relies on the fact that the scattering states are *supported* throughout the space, not just the CAP region. This will be illustrated further in the following.

We will now study the same type of spectra using the energy CAP of Eq. (10). We have chosen an CAP function of form

$$\mu(\varepsilon) = \mu_0 \sqrt[6]{\varepsilon}. \tag{19}$$

The energy distribution of the liberated and absorbed particle is now provided by Eq. (12), as opposed to Eq. (9) in the preceding case. The results are displayed for various values of μ_0 in the right column of Fig. 1. It differs from the ones in the left column in several respects. One difference is that these spectra are all strictly non-negative – in accordance with Eq. (12). A more striking difference is how strongly these spectra depend on the CAP strength μ_0. Specifically, ripples are not resolved at all at hard absorption, while the resolution of the structure improves as the absorption strength decreases. Although the spectra depend strongly on the CAP strength in this case, they do converge towards the same asymptotic form as in the former case.

These observations are concordant with the following picture: As a particle enters into the CAP region, with some probability, it is gradually attenuated and the energy of the absorbed part is recorded as dictated by Eq. (12). Suppose another outgoing wave reaches the energy CAP at a later stage; its energy contribution is, again, recorded and added to the total distribution – in an *incoherent* manner. Thus, these two waves are not allowed to interfere; absorption is detrimental to any interference patterns which would have emerged otherwise. The same would be the case if an energy detector placed in extreme vicinity with the quantum system induced a collapse in the wave function prior to interference. This loss in coherence together with the record of measured/absorbed data motivates how an energy-diagonal CAP simulates the action of a detector.

In more technical terms: When the measurement consist in projection onto the $|\varphi_\varepsilon\rangle$-basis, the pure state wave function is collapsed:

$$|\Psi\rangle\langle\Psi| \to \int d\varepsilon\, \zeta(\varepsilon) |\varphi_\varepsilon\rangle\langle\varphi_\varepsilon|, \tag{20}$$

where $\zeta(\varepsilon)$ is the distribution function for ε, the outcome of a series of energy measurements. This outcome may depend on the characteristics of the detector – where it is placed and how it is coupled to the system. Now, is it reasonable to interpret the energy distribution of Eq. (12), i.e., the energy-diagonal of the effective, accumulated density matrix σ_ε, as such a distribution function? Probability considerations require that the integral of $\zeta(\varepsilon)$ coincides with the trace of σ_ε; they should both equal the probability of the particle being unbound. Moreover, the distribution is calculated as a cumulative projective measurement onto states which are supported in the region of measurement/absorption only. And contributions picked up at different times should all contribute in a manifestly non-negative manner. The energy distribution of Eq. (12) does, in fact, comply with these criteria; it can be identified with a distribution function such as $\zeta(\varepsilon)$ of Eq. (20). Correspondingly, a CAP could act as an energy detector – iff it is diagonal in the basis of projection.

As we have seen, the situation is quite different when energy/momentum spectra are calculated using a local CAP, Eq. (8), instead. Here, the absorbed waves are projected onto states in which the CAP is *not* diagonal, states which are supported beyond the CAP region. According to Eq. (9), outgoing waves absorbed and recorded at different times are added

together in a *coherent* manner; effectively, they are allowed to interfere in momentum space also after absorption. Thus, even hard absorption allows interference patterns to be seen, and the emerging spectra turns out to be quite insensitive to the strength of the CAP function.

This suggests that in terms of implementation and simulation, local CAPs are numerically favourable for determining energy spectra as they allow for resolving fine structures while still admitting a strong truncation of the numerical domain. The energy CAP of Eq. (10), on the other hand, has the interesting trait that it simulates the effect of imposing a detector. Albeit experimental situations usually involve detectors placed far away and with very large extension, $R \to \infty$ and $\mu_0 \to 0^+$, we do find the ability to perform such dynamical studies to be an interesting one. As the CAP function $\mu(\varepsilon)$ could be virtually any positive function, there is a large degree of flexibility in modelling the detector and thus manipulate the quantum system in specific ways [13, 14].

B. Double slit interference

In the next example we will turn the table and use a local potential, Eq. (8), to model a detector instead. We will study the well known interference pattern emerging from a quantum particle passing through a double slit. An initial wave function with narrow spatial extension in the propagation direction travels towards a wall with two narrow gaps. Physically, the interference pattern that emerges on the other side of the slit will be altered if a wave emerging from one slit is subject to a position measurement before it has had time to overlap with waves emerging from the other slit.

Such a distortion is shown in the lower panel of Fig. 2. As illustrated in the upper panel, we have imposed a local CAP which is a two-dimensional analogue of Eq. (13) with a CAP function of the same form as in Eq. (18) – with x replaced by r, the distance from the midpoint between the two slits. The angular distribution of the absorbed particle is calculated form Eq. (15). In units defined by, again, setting $\hbar$ and the particle mass to one, the initial wave is travelling towards the wall with the mean de Broglie wavelength $\lambda = 2\pi/k = 2$; the initial width in the propagation direction is equal to λ. The slits, which have a rather smooth shape, are separated, centre to centre, by 20 length units, and their widths are both 1.5 units. The CAP strength $\gamma_0 = 0.03$.

As we see, the interference pattern is strongly affected by absorption close to the double slit, while it converges as the onset of the CAP is moved outwards. We explain this analogously to the case of the right column of Fig. 1: From Eq. (15) we see that absorbed waves are accumulated in an incoherent manner. Consequently, if a wave passing through one slit reaches the detector/CAP and is collapsed/absorbed before it has had time to overlap appreciably with waves emerging from the other slit, it will not be subject to the interference which would have taken place otherwise. Figure 3 serves to illustrate this.

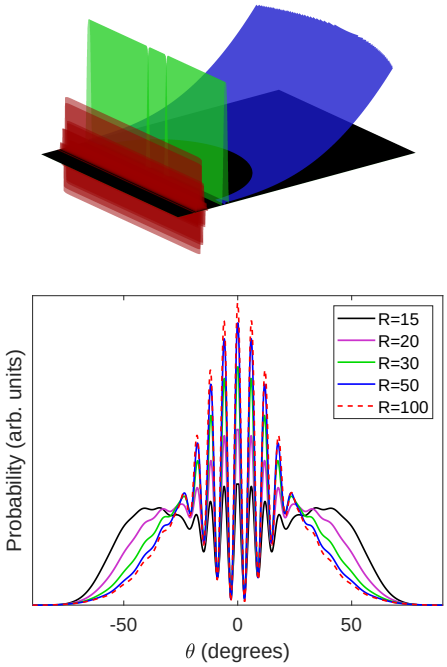

FIG. 2: Upper panel: The initial situation; a wave function of narrow spatial extension in the propagation direction (red) is incident on a high wall with two narrow gaps (green). At the other side, the outgoing waves are absorbed by a local CAP (blue). Lower panel: The angular interference pattern emerging from a particle passing through a double slit. It is obtained by probing the outgoing waves with absorbers placed at various distances from the double slit.

C. Concluding remarks

In the present work we have only considered one-particle systems. In [34] numerical examples similar to that of the left column of Fig. 1 are described with two particles instead of one. Contrary to the Schrödinger equation, Eq. (1), the GKLS equation, Refs. [42, 43], allows for maintaining the remaining particle as the other undergoes absorption [19, 44]. The remaining particle, which in general will not be in a pure state, is described by a density matrix ρ_1. This particle may go on to be absorbed as well and, thus, also contribute to an energy differential probability distribution. In both cases, i.e., in going from 2 to 1 particle and in going from 1 to 0 particles, the information about the removed particle may be aggregated as effective one-particle density matrices in a manner analogous to Eq. (5). Specifically, information from the first absorption is retained in the effective one-particle density matrix given by

$$d\sigma_{2\to 1} = \frac{1}{\hbar}\left\{\hat{\Gamma}, \Phi\right\} dt \quad \text{where} \tag{21a}$$

$$\Phi = 2\int\int dx dx'\, \phi(x,x')|x\rangle\langle x'| \quad \text{with} \tag{21b}$$

$$\phi(x,x';t) = \int dy\, \Psi_2(x,y;t)\Psi_2^*(x',y;t). \tag{21c}$$

Here $\Psi_2(x,y)$ is the wave function of the two-particle part, which remains a in a pure state. The second absorption is

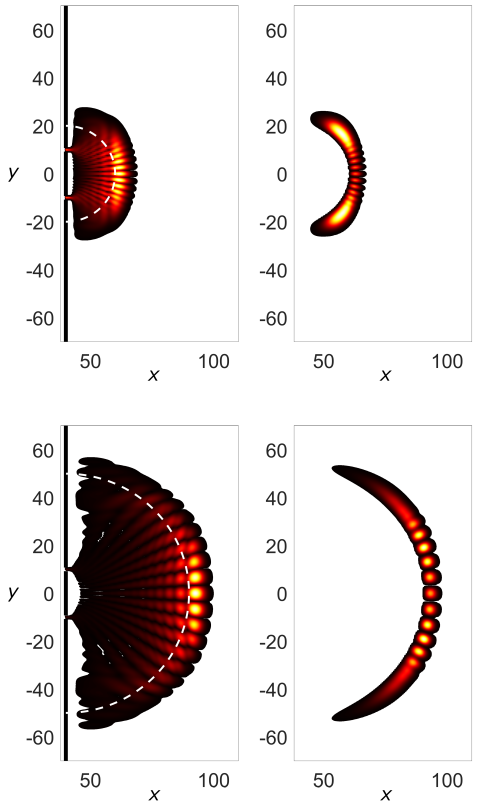

FIG. 3: The left panels show snapshots of the part of the wave function which has travelled through the double slit. Its initial momentum points in the x-direction. The length units in both the x and y directions are defined by setting $\hbar$ and the particle mass to unity. The wave packet is subject to an absorber with an onset R indicated by the white dashed curve; the upper case corresponds to $R = 20$ while $R = 50$ for the lower panels. The thick black lines to the left illustrates the wall. As the wave packet enters the absorption region, the amount of absorption at each position is aggregated. The right panels illustrates this aggregation. The interference patterns shown in the lower panel of Fig. 2 is precisely this distribution – with the radial distance r integrated out, see Eq. (15).

recorded via

$$d\sigma_{1\to 0} = \frac{1}{\hbar}\left\{\hat{\Gamma}, \rho_1\right\} dt, \tag{22}$$

where ρ_1, as mentioned, is the one-particle sub-system emerging from the first absorption. The effective one particle density matrix Φ in Eq. (21b) may conveniently be expressed in terms of second quantization, see Ref. [34] for details. Both these effective density matrices, i.e., $\sigma_{2\to 1}$ and $\sigma_{1\to 0}$, may be analysed on the fly by continuous projective measurements in the exact same manner as explained in Sec. II.

This also applies to energy-absorbers, Eq. (10), as also these may expressed as one-particle operators in a multi-particle context. Thus, the arguments presented here on the correspondence between CAPs and detectors are not limited to the one-particle case.

It should be stressed that neither the idea of CAPs as detectors nor the general idea of using CAPs actively to probe outgoing waves is not unprecedented in literature. In [27] it was explained how different decay products in a breakup process may be distinguished via matrix elements explicitly involving CAP functions. This method, which has the advantage of being apt for implementation within the *Multi-Configurational Time-Dependent Hartree* approximation [45], exploits the possibility of assigning different CAPs to the various decay channel.

Another technique used for analyzing unbound particles encountered in literature is referred to as *virtual detectors*, see, e.g., [21, 22]. In the present context, the naming calls for some disambiguation. Along with a number of similar techniques, see, e.g., [23–25], it involves the calculation of the probability current, or *flux*, through some surface. While the notion of a detector would, to some extent, seem adequate also in this context, *virtual detectors* differ more from the present framework than the name would suggest. One reason for this is that, contrary to the CAP, the *virtual detector* does not have any spatial extension, nor does it bring about any loss in coherence. The CAP is simply used in order to attenuate outgoing waves; contrary to the method discussed above and the one presented here, it is not used to *probe* the outgoing wave. Moreover, it does not seem to generalize naturally to the multi-particle case.

Yet another approach for modelling detection by means of an absorbing boundary is proposed in [20], which, in turn, is partially based on the work of [18]. As in the case of the *virtual detector* it introduces a detector model without extension. In contrast to most other works involving CAPs, however, the absorber itself is also without extension. Correspondingly, the system is subject to pronounced reflection at the boundary. And the proposed *detection* is not necessarily accompanied with absorption – in stark contrast with the notion of detection in the present work.

On the other hand, the *Monte Carlo Wave Packet* approach and the closely related *Quantum Jump* method, see, e.g., Refs. [46, 47], bear strong resemblance to the present approach. Such approaches, along with the derivation of Halliwell [13], could hopefully assist in making a closer correspondence between physical detectors and the shape of the CAP functions, be it of the form of Eq. (8), Eq. (10) or any other.

IV. CONCLUSIONS

We explained how CAPs, in addition to attenuating outgoing waves, may be used to *probe* quantum particles undergoing absorption. By theoretical derivations and numerical examples we demonstrated how differential spectra of unbound particles, such as energy distributions or angular distributions, could be determined. We made a clear distinction between situations in which the absorbed particle is analysed by projection onto states in which the absorbing potential is diagonal and situations when it is non-diagonal.

In the latter case, we showed that energy spectra are quite insensitive to the shape of local CAP as it allows for waves absorbed at different times to interfere. This is not the case in

the former, diagonal case. In such situations the CAP acts as a detector. This applies both to the fact that the CAP effectively provides distribution functions for absorbed particles – and to the fact that it proves detrimental to interference effects in these distribution functions.

This, in turn, may open an avenue for studying how quantum systems may be manipulated by tailored detection.

[1] V. Weisskopf and E. Wigner, Zeit.Phys. **63**, 54 (1930).
[2] R. Kosloff and D. Kosloff, J. Comput. Phys. **63**, 363 (1986).
[3] U. V. Riss and H. D. Meyer, J. Phys. B **26**, 4503 (1993).
[4] J. Muga, J. Palao, B. Navarro, and I. Egusquiza, Phys. Rep. **395**, 357 (2004).
[5] R. Santra and L. S. Cederbaum, J. Chem. Phys. **117**, 5511 (2002).
[6] R. Lefebvre, M. Sindelka, and N. Moiseyev, Phys. Rev. A **72**, 052704 (2005).
[7] R. Santra, Phys. Rev. A **74**, 034701 (2006).
[8] A. del Campo, F. Delgado, G. García-Calderón, J. G. Muga, and M. G. Raizen, Phys. Rev. A **74**, 013605 (2006).
[9] T.-C. Jagau, D. Zuev, K. B. Bravaya, E. Epifanovsky, and A. I. Krylov, J. Chem. Phys. Lett. **5**, 310 (2014).
[10] G. Allcock, Ann. Phys. **53**, 253 (1969).
[11] G. Allcock, Ann. Phys. **53**, 286 (1969).
[12] G. Allcock, Ann. Phys. **53**, 311 (1969).
[13] J. Halliwell, Prog. Theor. Phys. **102**, 707 (1999).
[14] L. S. Schulman, Phys. Rev. A **57**, 1509 (1998).
[15] J. Echanobe, A. del Campo, and J. G. Muga, Phys. Rev. A **77**, 032112 (2008).
[16] J. G. Muga, J. Echanobe, A. del Campo, and I. Lizuain, J. Phys. B **41**, 175501 (2008).
[17] A. Ruschhaupt, J. A. Damborenea, B. Navarro, J. G. Muga, and G. C. Hegerfeldt, Europhys. Lett. **67**, 1 (2004).
[18] R. Werner, in *Annales de l'IHP Physique théorique* (1987), vol. 47, pp. 429–449.
[19] S. Kvaal, Phys. Rev. A **84**, 022512 (2011).
[20] R. Tumulka, Ann. Phys. **442**, 168910 (2022).
[21] B. Feuerstein and U. Thumm, J. Phys. B **36**, 707 (2003).
[22] X. Wang, J. Tian, and J. H. Eberly, J. Phys. B **51**, 084002 (2018).
[23] A. M. Ermolaev, I. V. Puzynin, A. V. Selin, and S. I. Vinitsky, Phys. Rev. A **60**, 4831 (1999).
[24] S. Selstø, M. Førre, J. P. Hansen, and L. B. Madsen, Phys. Rev. Lett. **95**, 093002 (2005).
[25] L. Tao and A. Scrinzi, New J. Phys. **14**, 013021 (2012).
[26] A. Scrinzi, New J. Phys. **14**, 085008 (2012).
[27] A. Jäckle and H. D. Meyer, J. Chem. Phys. **105**, 6778 (1996).
[28] S. Chelkowski, C. Foisy, and A. D. Bandrauk, Phys. Rev. A **57**, 1176 (1998).
[29] R. Grobe, S. Haan, and J. Eberly, Comput. Phys. Commun. **117**, 200 (1999).
[30] M. Lein, E. K. U. Gross, and V. Engel, Phys. Rev. Lett. **85**, 4707 (2000).
[31] X. M. Tong, K. Hino, and N. Toshima, Phys. Rev. A **74**, 031405(R) (2006).
[32] U. De Giovannini, D. Varsano, M. A. L. Marques, H. Appel, E. K. U. Gross, and A. Rubio, Phys. Rev. A **85**, 062515 (2012).
[33] D. A. Tumakov, D. A. Telnov, G. Plunien, V. A. Zaytsev, and V. M. Shabaev, Eur. Phys. J. D **74**, 188 (2020).
[34] S. Selstø, Phys. Rev. A **103**, 012812 (2021).
[35] A. Sergi, Atti della Accademia Peloritana dei Pericolanti-Classe di Scienze Fisiche, Matematiche e Naturali **97**, 11 (2019).
[36] D. C. Brody and E.-M. Graefe, Phys. Rev. Lett. **109**, 230405 (2012).
[37] J. Cornelius, Z. Xu, A. Saxena, A. Chenu, and A. del Campo, arXiv p. 2108.06784 (2021).
[38] U. V. Riss and H. D. Meyer, J.Phys. B **28**, 1475 (1995).
[39] U. V. Riss and H. D. Meyer, J. Phys. B **31**, 2279 (1998).
[40] N. Moiseyev, J. Phys. B **31**, 1431 (1998).
[41] A. Scrinzi, Phys. Rev. A **81**, 053845 (2010).
[42] V. Gorini, A. Kossakowski, and E. Sudarshan, J. Math. Phys. **17**, 821 (1976).
[43] G. Lindblad, Comm. Math. Phys. **48**, 119 (1976).
[44] S. Selstø and S. Kvaal, J. Phys. B **43**, 065004 (2010).
[45] M. Beck, A. Jäckle, G. Worth, and H.-D. Meyer, Phys. Rep. **324**, 1 (2000).
[46] J. Dalibard, Y. Castin, and K. Mølmer, Phys. Rev. Lett. **68**, 580 (1992).
[47] G. C. Hegerfeldt and M. B. Plenio, Phys. Rev. A **47**, 2186 (1993).